



**Environmental  
Science**  
Water Research & Technology

**Modeling SARS-CoV-2 RNA Degradation in Small and Large Sewersheds**

Journal:	<i>Environmental Science: Water Research &amp; Technology</i>
Manuscript ID	EW-ART-10-2021-000717.R1
Article Type:	Paper

SCHOLARONE™  
Manuscripts

## Modeling SARS-CoV-2 RNA Degradation in Small and Large Sewersheds

<sup>1</sup>Camille McCall, <sup>2</sup>Zheng N. Fang, <sup>2</sup>Dongfeng Li, <sup>2</sup>Andrew J. Czubai, <sup>1</sup>Andrew Juan, <sup>1</sup>Zachary LaTurner, <sup>3</sup>Katherine Ensor, <sup>3,4</sup>Loren Hopkins, <sup>1</sup>Phil Bedient, <sup>\*1</sup>Lauren B. Stadler

<sup>1</sup>Department of Civil and Environmental Engineering, Rice University, Houston, TX, 77005

<sup>2</sup>Department of Civil Engineering, The University of Texas at Arlington, Arlington, TX, 76019

<sup>3</sup>Department of Statistics, Rice University, Houston, TX, 77005

<sup>4</sup>Houston Health Department, 8000 N. Stadium Dr., Houston, TX, 77054

\*Corresponding Author: Lauren Stadler

Mailing address:

6100 Main Street, MS-519

Houston, TX 77005

Email: [lauren.stadler@rice.edu](mailto:lauren.stadler@rice.edu)

**Water Impact Statement:** Microbial decay in sewer collection systems poses a significant challenge for wastewater-based epidemiology (WBE) for COVID-19 among other diseases. This work facilitates the understanding of SARS-CoV-2 decay in small and large sewersheds and under various wastewater temperatures. With this information we proposed a novel approach to designing a reliable and sustainable sampling infrastructure for WBE.

## 1                    **Modeling SARS-CoV-2 RNA Degradation in Small and Large Sewersheds**

2  
3        <sup>1</sup>Camille McCall, <sup>2</sup>Zheng N. Fang, <sup>2</sup>Dongfeng Li, <sup>2</sup>Andrew J. Czubai, <sup>1</sup>Andrew Juan, <sup>1</sup>Zachary  
4                    LaTurner, <sup>3</sup>Katherine Ensor, <sup>3,4</sup>Loren Hopkins, <sup>1</sup>Phil Bedient, <sup>\*1</sup>Lauren B. Stadler

5  
6  
7        <sup>1</sup>Department of Civil and Environmental Engineering, Rice University, Houston, TX, 77005

8        <sup>2</sup>Department of Civil Engineering, The University of Texas at Arlington, Arlington, TX, 76019

9        <sup>3</sup>Department of Statistics, Rice University, Houston, TX, 77005

10        <sup>4</sup>Houston Health Department, 8000 N. Stadium Dr., Houston, TX, 77054

11  
12        \*Corresponding Author: Lauren Stadler

13        Mailing address:

14        6100 Main Street, MS-519

15        Houston, TX 77005

16        Email: lauren.stadler@rice.edu

### 17 18        **Abstract**

19        Wastewater-based epidemiology has played a significant role in monitoring the COVID-19  
20        pandemic, yet little is known about degradation of SARS-CoV-2 in sewer networks. Here, we  
21        used advanced sewershed modeling software to simulate SARS-CoV-2 RNA degradation in  
22        sewersheds across Houston, TX under various temperatures and decay rates. Moreover, a novel  
23        metric, population times travel time (PT), was proposed to identify localities with a greater  
24        likelihood of undetected COVID-19 outbreaks and to aid in the placement of upstream samplers.  
25        Findings suggest that travel time has a greater influence on RNA degradation across the  
26        sewershed as compared to temperature. SARS-CoV-2 RNA degradation at median travel times

27 was approximately two times greater in 20°C wastewater between the small sewershed,  
28 Chocolate Bayou, and the larger sewershed, 69th Street. Lastly, placement of upstream samplers  
29 according to the PT metric can provide a more representative snapshot of disease incidence in  
30 large sewersheds. This study helps to elucidate discrepancies between SARS-CoV-2 viral load in  
31 wastewater and clinical incidence of COVID-19. Incorporating travel time and SARS-CoV-2  
32 RNA decay can improve wastewater surveillance efforts.

33

34 **Keywords:** COVID-19, Wastewater-based epidemiology, Coronaviruses, Decay, Travel time

35

## 36 **1. Introduction**

37

38 Municipal wastewater treatment plants collect untreated wastewater from communities ranging  
39 from hundreds to millions of inhabitants per day within a given sewershed. This wastewater can  
40 be scrutinized to obtain critical insights into biological and chemical markers that are reflective  
41 of community health within the serviced population, an approach known as wastewater-based  
42 epidemiology (WBE).

43

44 In WBE, untreated wastewater is considered analogous to a population-wide urine and stool  
45 sample. This representative sample can be used to evaluate community health and the prevalence  
46 of certain diseases by directly measuring markers of concern. Viral monitoring in wastewater has  
47 gained much attention considering that viruses do not replicate independent of a host cell and are  
48 persistent in the environment. Several viral pathogens including hepatitis A virus, hepatitis E

49 virus, norovirus, sapovirus, astrovirus, and poliovirus have been monitored in wastewater for  
50 community health tracking (1–5).

51  
52 Recently, WBE has been recognized as a promising tool for tracking SARS-CoV-2, the causative  
53 agent of Coronavirus Disease 2019 (COVID-19). SARS-CoV-2 is an enveloped positive-sense  
54 RNA virus belonging to the *Coronaviridae* family. Although the primary transmission route of  
55 SARS-CoV-2 is via respiratory droplets, evidence of fecal shedding of SARS-CoV-2 in infected  
56 individuals has led to the global attention of WBE in the ongoing fight against COVID-19 (6).  
57 Several studies have highlighted the potential for viral signals to precede clinical cases and  
58 capture the extent of asymptomatic individuals that are not reported in health care facilities (7–  
59 10).

60 Generally, evidence supports the utility of WBE as a public health and environmental tracking  
61 tool for viral disease outbreaks. Still, in some cases discrepancies exist between viral signal in  
62 wastewater and disease prevalence, specifically with SARS-CoV-2 (11).

63  
64 Viral measurements from wastewater alone may not be sufficient for disease tracking.  
65 Considerations such as the environmental matrix, sampling regimen, sewer collection system,  
66 viral stability, and disease characteristics are critical aspects to establishing correlations between  
67 viral signal and disease incidence in the community (12). Among these critical considerations is  
68 the stability of the virus and its genetic material in the sewershed. Microbial degradation plays a  
69 significant role in determining what proportion of RNA shed in feces gets captured at the outfall  
70 of a wastewater treatment plant (WWTP). To date, few studies have investigated RNA  
71 degradation of SARS-CoV-2 in wastewater (13–16).

72

73 In two of the studies, temperature had a significant influence on variations between first-order  
74 decay rates (11,13). Temperature was also found to have a greater impact on RNA degradation  
75 than the sample matrix (15). Despite the agreement on the importance of temperature between  
76 the two studies, Weidhaas et al., 2021 obtained a significantly higher decay constant ( $4.32 \text{ day}^{-1}$ )  
77 at  $35^\circ\text{C}$  than Ahmed et al., 2020 ( $0.24 \text{ day}^{-1}$ ) at  $37^\circ\text{C}$  for similar gene targets. This indicates that  
78 there are other factors that have a notable influence on RNA degradation such as sample  
79 preparation or wastewater composition. A recent study demonstrated that the abundance of the  
80 SARS-CoV-2 N1 marker is associated with total organic carbon and pH (17). Furthermore,  
81 Bivins et al. 2020 evaluated changes in decay constants when the starting viral titer was low as  
82 compared to high titers. Low titers ( $10^3 \text{ TCID}_{50} \text{ mL}^{-1}$ ) obtained a decay constant of  $0.09 \text{ day}^{-1}$  at  
83  $20^\circ\text{C}$  which was significantly lower than that of the high titer ( $10^5 \text{ TCID}_{50} \text{ mL}^{-1}$ ) at the same  
84 temperature,  $0.67 \text{ day}^{-1}$ .

85

86 From these studies it is evident that further work is needed to understand degradation of SARS-  
87 CoV-2 under various conditions. Moreover, only one study to date has explored degradation of  
88 SARS-CoV-2 in sewer systems using a first-order decay rate derived from a study on the  
89 infectivity of various coronaviruses in wastewater after 21 days (16,18). The authors found that  
90 larger sewersheds further confound the effects of temperature on degradation. Indeed, it is  
91 expected that longer travel times will create notable discrepancies between viral concentration  
92 and COVID cases in communities. Furthermore, since upstream sampling provides high spatial  
93 resolution and is more representative of the sampled population (16,19), the placement of  
94 wastewater samplers in sewersheds remains an ongoing area of interest (20,21). Yet, to our

95 knowledge, no quantitative approaches for selecting upstream sampling locations to capture  
96 outbreaks and minimize degradation of SARS-CoV-2 RNA have been proposed.

97  
98 Upstream sampling refers to sampling within the sewer system from locations such as manholes,  
99 as compared to sampling at the influent of a WWTP (downstream sampling). Several studies  
100 have implemented upstream sampling for monitoring COVID-19 outbreaks in hospitals (22),  
101 universities (23), and metropolitan neighborhoods (24). There are practical constraints that  
102 dictate the selection of upstream sites, namely available resources, accessibility, and safety.  
103 Moreover, sampling site selection based on travel time should be considered to further increase  
104 the impact of upstream sampling on WBE outcomes.

105  
106 Interestingly, Haak et al. 2022 found population density to be highly significant when comparing  
107 SARS-CoV-2 RNA concentrations in wastewater between different neighborhoods within the  
108 same sewershed. Though the effects of population density on SARS-CoV-2 stability in  
109 wastewater are not fully understood, population density remains a significant factor in epidemics  
110 and can facilitate the rate at which a disease disseminates within a community. A recent study  
111 found population density to have a positive effect on the basic reproductive number ( $R_0$ ) of  
112 COVID-19 with  $R_0$  increasing by an average of .11 when population density doubled (25).  
113 Likewise, a study assessing the effect of several environmental and geographical factors on  
114 COVID-19 cases found population density to be the best predictor of cases when looking at 81  
115 provinces in Turkey (26). Consequently, the higher the population density, the more potential  
116 there is for a disease outbreak. Considering its significance, population density can be a critical

117 component for identifying sampling locations based on potential hotspots for rapid disease  
118 spread.

119

120 Here, we model SARS-CoV-2 RNA degradation in sewersheds across Houston that vary in  
121 service population and geographic area based on published and experimentally derived first-  
122 order decay rates, wastewater temperature, and sewershed travel times. Finally, we propose a  
123 novel metric for determining critical locations for placing upstream samplers to improve SARS-  
124 CoV-2 monitoring in wastewater.

125

## 126 **2. Materials and Methods**

127

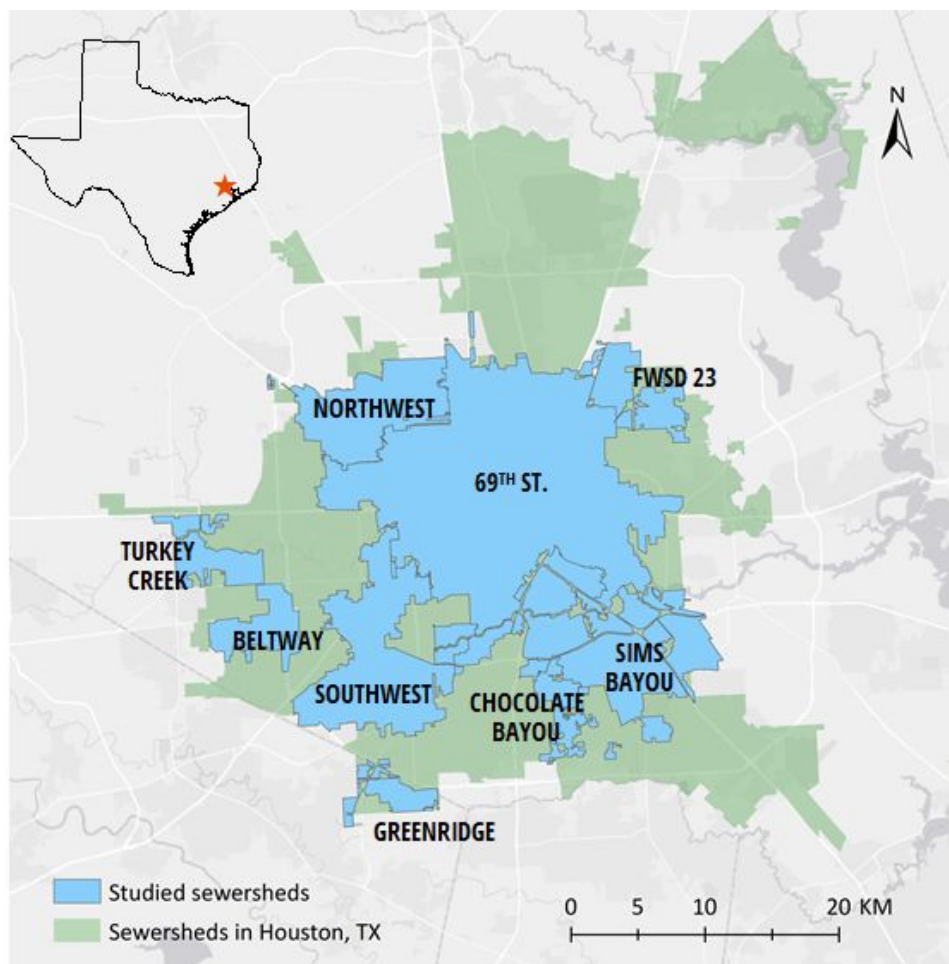
### 128 **2.1. Study Area and Overview**

129

130 Houston has 39 sewersheds with a total service area covering approximately 1,451 km<sup>2</sup> (358,580  
131 acres). Of those, ten sewersheds were selected for this study based on the availability of  
132 sewershed hydraulic models provided by Houston Public Works. The location and characteristics  
133 of the selected sewersheds are detailed in **Figure 1** and **Table S1**, respectively. Hydraulic  
134 modeling was conducted to simulate performance metrics which were then used to compute  
135 travel times for each sewershed. Multiple SARS-CoV-2 decay rates based on published and  
136 experimental studies were then used with the computed travel times to estimate viral RNA  
137 degradation in the sewersheds.

138





139

140

141 **Figure 1.** Ten selected wastewater treatment plant service areas (sewersheds) are shown in blue.

142 Sims Bayou has overlapping service areas recognized as Sims Bayou North and South

143 sewersheds. The remainder of Houston's sewersheds are shown in green.

144

## 145 2.2. Sewershed Modeling

146

147 Hydraulic modeling of sewersheds in this study was accomplished using the Infoworks ICM

148 software (ICM stands for Integrated Catchment Modeling). Developed by Innowyze®,

149 Infoworks ICM is a hydrodynamic model capable of simulating the hydrology and hydraulics

150 of aboveground surfaces as well as underground drainage networks based on the conservation  
151 of mass and momentum. Due to its robustness and versatility, Infoworks ICM has been used by  
152 numerous municipalities, like the City of Houston, for stormwater, flood control infrastructure,  
153 and sewer management.

154

155 In this study, Infoworks ICM models for ten sewersheds were obtained from the City of  
156 Houston Public Works department. Each model represents the wastewater network and service  
157 areas for a sewershed. The models were calibrated by Houston Public Works under dry and  
158 wet weather conditions. At a minimum, two rainfall events are used for model calibration and  
159 one event for verification. A previous study applied a similar approach using an Infoworks  
160 ICM model and obtained strong correlations between observed and simulated water levels in a  
161 pumping station during a rainfall event (27). Infoworks ICM provides separate solution  
162 models for permeable planes, force mains, pressurized pipes or normal gravity flow. An ICM  
163 model consists of a network of links and nodes, in which the links represent pipes or conduits,  
164 and the nodes represent manholes or other control structures (e.g., outfall or WWTP).  
165 Additionally, the model allows for either one or multiple outfall locations. Based on the  
166 connectivity of the nodes and links, service areas that drain to any particular node could be  
167 further separated into individual subcatchments. The gradient or slope of the link is calculated  
168 using the provided starting and ending invert elevations.

169

170 ICM divides each conduit into a number of discrete computational points and regularly-spaced  
171 segments with intervals that are 20 times the pipe diameter. Flow, velocity, and other  
172 performance metrics are computed in each segment. Inflow can be added to certain nodes as

173 point sources, but in this study, diurnal curves in the form of wastewater profiles with hourly  
174 time steps were applied at corresponding subcatchments to represent wet and dry conditions.  
175 With specified information of population and per capita flow, the wastewater profile can be  
176 developed from a calibrated model and is designed to mimic dry weather flow as typically seen  
177 during flow monitoring.

178

### 179 **2.3. Computing Travel Time**

180

181 While various performance metrics such as head, flow, velocity, volume, and water depth are  
182 computed by ICM, individual travel times for subcatchments are not. In a typical wastewater  
183 system, the conduits are connected to a common outfall, which usually represents the local  
184 WWTP. All model networks must have at least one common outfall, but networks are allowed to  
185 have multiple outfalls which could represent wet-weather overflows, emergency bypasses, or  
186 pump stations to a different wastewater system. Because there is not always a single common  
187 outfall, a structured query language (SQL) script was developed to allow users to specify a  
188 terminal point. Having terminal points enables travel time to be computed from any  
189 subcatchment to the specified points. The user determines the number of iterations for the query,  
190 the minimum assumed velocity, and the specific simulation time that the query would run. The  
191 query then uses the trace tool, which selects all upstream conduits, nodes, and subcatchments to a  
192 specified point and iterates the simulated results to determine a corresponding travel time based  
193 on the cumulative conduit length travelled and velocity at the given point. In the case where  
194 multiple flow paths exist, the query assumes that wastewater would always travel on the shortest  
195 path, therefore computing the shortest travel time from the point of entry to the terminal point.

196 Lastly, the computed travel times for the entire model network were then exported into GIS for  
197 further analysis.

198

#### 199 **2.4. Identifying Decay Rate Studies**

200

201 A literature search was conducted in October 2020 and again in February 2021 using Web of  
202 Science and Google Scholar databases to identify studies with first-order degradation rates for  
203 SARS-CoV-2 RNA. SARS-CoV-2 was used as a keyword paired with one or more of the  
204 following: wastewater, degradation, decay, sewershed, persistence, fate, and survivability. The  
205 criteria for inclusion were (1) peer-viewed journal articles (excluded reviews, metadata, pre-  
206 prints, editorial material), (2) a focus on SARS-CoV-2 in untreated wastewater samples or  
207 simulated untreated wastewater, (3) includes at least one original, experimentally determined  
208 decay rate for SARS-CoV-2 RNA.

209

#### 210 **2.5. Decay of SARS-CoV-2 RNA in Sewage**

211

212 Along with experimentally determined decay rates of SARS-CoV-2 from published literature,  
213 decay rates were also generated. To determine decay rates for SARS-CoV-2 RNA, roughly 1  
214 gallon of wastewater influent was collected from a 24-hour composite sampler and transported  
215 on ice to Houston Public Works central processing laboratory. Approximately 500 mL of  
216 wastewater was collected in triplicate, stored in Nalgene bottles, and transported on ice to Rice  
217 University. The 500 mL bottles were weighed to accurately determine the volume of wastewater  
218 in each bottle. Next, each sample was poured into a sterilized 1 L Erlenmeyer flask containing a

219 stir bar. Flasks were loosely capped with aluminum foil to prevent evaporation and placed on a  
220 stir plate at the lowest possible setting to maintain a heterogenous mixture.

221

222 A 50 mL sample was immediately collected from each flask and concentrated via the HA  
223 filtration method with bead beating as previously described here (28). HA filters were stored at -  
224 80°C. Wastewater from each flask was collected, concentrated, and stored via this method every  
225 24 hours for the next 6 days. All wastewater samples were incubated at room temperature  
226 (~20°C) in a Biosafety cabinet. After the 6 days, all stored samples were simultaneously  
227 extracted using the Qiagen Allprep Powerviral DNA/RNA kit (Qiagen) with some modifications  
228 to the manufacturer's protocol. Briefly, 7 µL of β-Mercaptoethanol and 693 µL of PM1 solution  
229 were added to each bead tube containing the sample filters. Samples were then bead beaten at  
230 3,500 rpm in a Mini-Beadbeater 24 (BioSpec) for 1 min, cooled on ice for 2 min, and bead  
231 beaten once more for 1 min. Following bead beating, samples were centrifuged at 17,000 g for 2  
232 min. Roughly 450 µL of sample lysate was extracted from each bead tube and transferred to a  
233 QIAcube Connect (Qiagen) for automated extraction. Samples were eluted in 50 µL of nuclease-  
234 free water, stored at -20°C, and processed within 24 hours.

235

236 SARS-CoV-2 N1 and N2 gene targets were quantified in wastewater extracts using a previously  
237 described method (28). In short, a duplex reverse transcriptase digital droplet PCR (RT-ddPCR)  
238 was carried out using the One-Step RT-ddPCR Advanced kit for probes (Bio-Rad) on a QX200  
239 AutoDG Droplet Digital PCR System (Bio-Rad) according the manufacturer's recommendations.  
240 Ten microliters of RNA extract, no template control, or positive control was transferred to a 12 µ  
241 L reaction mix containing final concentrations of 900 nmol of each primer and 250 nmol for each

242 probe. All reactions were performed in triplicate with thermocycling conditions detailed here  
243 (28). Samples were then read on a QX200 Droplet Reader (Bio-Rad) and analyzed using the  
244 QuantaSoft v1.7.4 software. The limit of quantification (LOQ) was previously determined as  
245 0.767 gene copies/ $\mu\text{L}$  of RNA according to a threshold of 3 positive droplets per 10,000 total  
246 droplets as recommended by the manufacturer. A linear regression analysis was performed in R  
247 (29) to determine the decay rates for each target. Concentrations of SARS-CoV-2 were log-  
248 transformed to satisfy the assumptions of normality according to a visual inspection of the  
249 quantile-quantile (Q-Q) plots.

250

## 251 **2.6. Estimation of SARS-CoV-2 RNA Degradation in Sewersheds Based on First-** 252 **order Decay**

253

254 To the best of our knowledge, all experimentally-derived published decay rates for SARS-CoV-2  
255 were included in this study. A temperature of 20°C was used to compare the influence of each  
256 decay rate on the proportion of virus loss in select sewersheds across studies. The following  
257 formula is an approximation of the Arrhenius equation used to determine the dependence of first-  
258 order rates on temperature (16,30,31):

259

$$260 \quad \frac{k_2}{k_1} = Q_{10}^{(T_2 - T_1)/10} \quad (1)$$

261

262 where  $Q_{10}$  is the temperature coefficient,  $k_1$  and  $k_2$  are the lower and upper decay rate constants,  
263 respectively, and  $T_1$  and  $T_2$  are the temperatures in Celsius for the upper and lower rate  
264 constants, respectively. The temperature coefficient  $Q_{10}$  is the factor by which a rate changes

265 given a ten degree increase in temperature and is usually between 2 and 3 for biological systems  
266 (31,32).

267

268 Eq (1) was used to estimate the decay rate at 20°C for the Weidhaas et al., 2021 study, using the  
269 decay rates measured at 10 and 35°C. The temperature-dependent linear regression equation  
270 reported by the authors was used to determine the decay rate of SARS-CoV-2 RNA at 20°C for  
271 Ahmed et al., 2020.

272

273 The degradation of SARS-CoV-2 in the sewershed over time is expected to follow exponential  
274 decay as expressed in eq (2) where  $C(t)$  is the concentration of SARS-CoV-2 after time  $t$ ,  $C_0$  is  
275 the initial concentration of SARS-CoV-2 released in the wastewater, and  $k$  is the first order  
276 decay rate.

277

$$278 \quad \frac{C(t)}{C_0} = e^{-kt} \quad (2)$$

279

280 Assuming an initial viral RNA proportion of 1 or 100%, eq (2) was substituted into eq (3) to  
281 estimate the proportion of SARS-CoV-2 RNA loss (L) eq (4) or remaining (R) eq (5) at a given  
282 time within the sewershed.

283

$$284 \quad \textit{Proportion degraded} = 1 - \frac{C(t)}{C_0} \quad (3)$$

285

$$286 \quad L = 1 - e^{-kt} \quad (4)$$

287

288 
$$R = 1 - L \tag{5}$$

289

290 The half-life  $t_{\frac{1}{2}}$  and  $t_{90}$  (the time for viral load to decrease by one log unit) for each decay rate  $k$   
291 were obtained from the published work or derived from the following formulas, respectively:

292

293 
$$t_{\frac{1}{2}} = \frac{\ln(2)}{k} \tag{6}$$

294 
$$t_{90} = \frac{-\ln(0.1)}{k} \tag{7}$$

295

## 296 **2.7. PT Metric for Identifying Hotspots**

297

298 Aside from using travel time isochrones to determine the spatial distribution of viral RNA signal,  
299 they could also be used in conjunction with population density information to help identify  
300 potential viral hotspot areas. In this study, a normalized population times travel time (PT) metric  
301 is introduced to identify critical locations for placing upstream samplers. Normalized PT maps  
302 for the 69th Street sewershed were generated by multiplying population density information (P)  
303 in each sub-sewershed area by their corresponding travel times (T), and then normalized by the  
304 maximum PT value computed for the 69th Street and Chocolate Bayou sewersheds. The  
305 resulting normalized PT maps have values that range from 0 (0%) to 1 (100%). Areas with low  
306 PT values indicate a low likelihood of an undetected outbreak, due to low population density,  
307 short travel times, or both. Conversely, areas with high PT values imply a higher likelihood of  
308 undetected outbreaks. This is especially true for areas with the highest PT values (i.e., at or close  
309 to 100%), signifying that those areas have both high population density and long travel times.

310



### 311        **3. Results and Discussion**

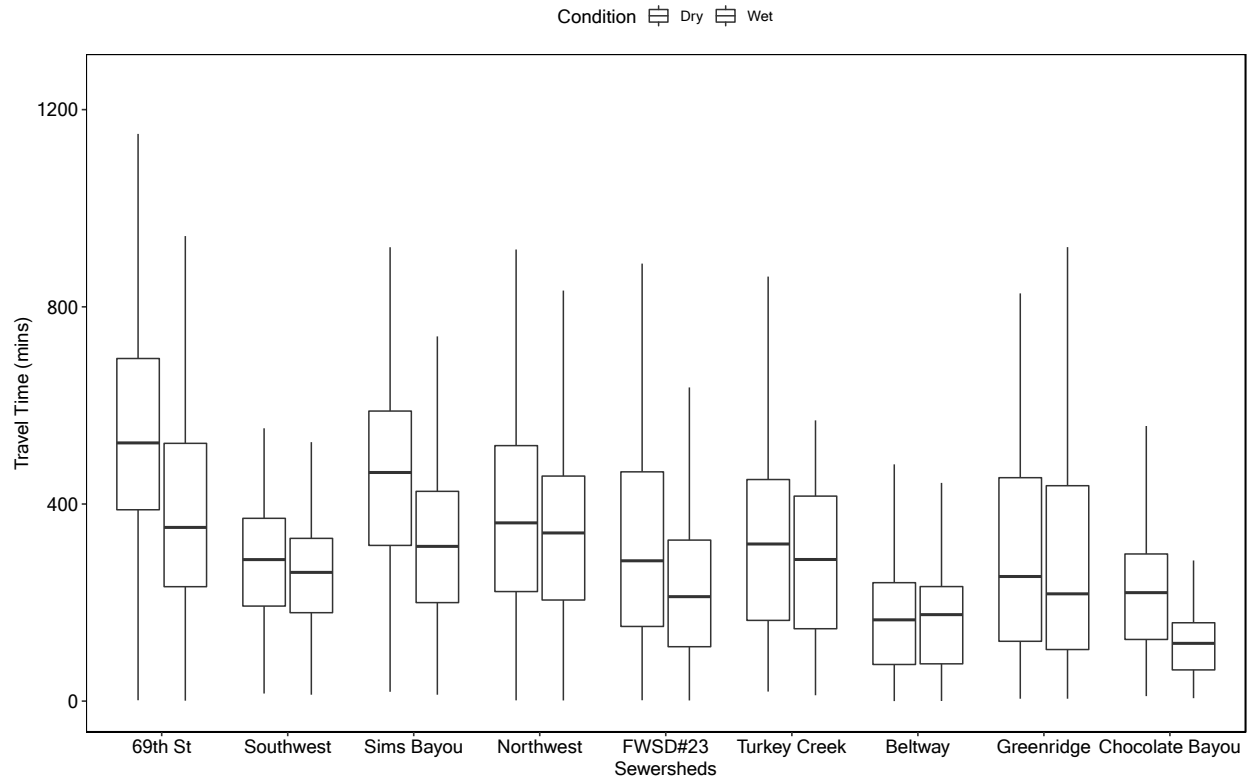
312

#### 313        **3.1. Impact of Weather Conditions on Wastewater Travel Time in Sewersheds**

314

315        To assess the impact of wet weather on travel times, the ICM model was used to compute travel  
316        times under wet and dry conditions for each sewershed (**Figure 2**). Travel times under dry  
317        weather conditions were generally higher than wet conditions. The 69th Street and Chocolate  
318        Bayou sewersheds were used for further analysis due to the differences in characteristics, and  
319        because they represented the sewersheds with the largest and smallest service areas studied,  
320        respectively.

321        Median dry weather travel times for 69th Street and Chocolate Bayou were 523 min (s.d. =  
322        217.58 min) and 220 min (s.d.= 152.12 min) with a comparable maximum dry weather travel  
323        time of 1207 mins and 1123 mins, respectively (**Figure 3**).



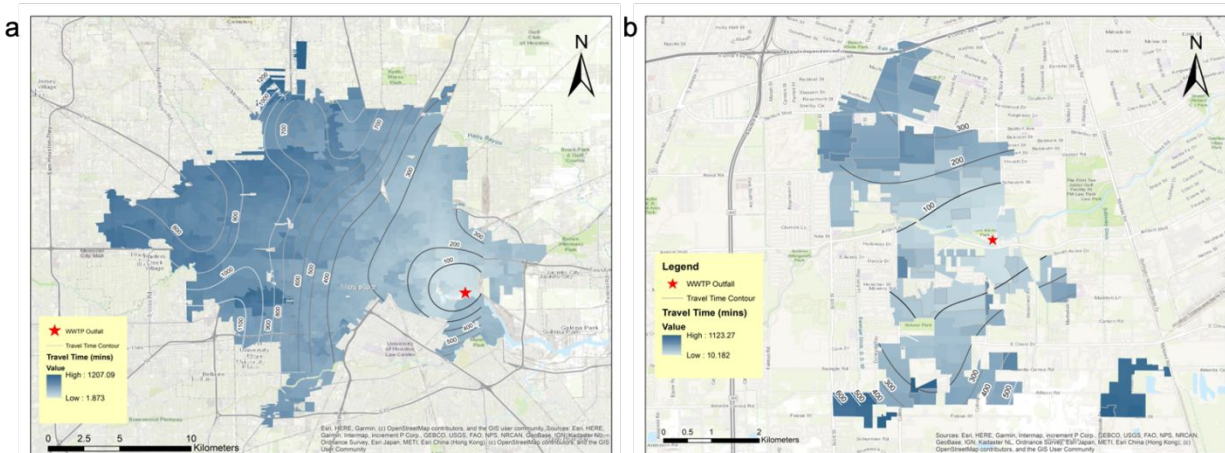
324

325 **Figure 2.** Boxplot of travel times for select sewersheds under dry and wet weather conditions.

326 Horizontal lines represent the median travel time. Lower and upper whiskers represent the 25<sup>th</sup>

327 and 75<sup>th</sup> percentiles, respectively.

328



329

330 **Figure 3.** Heat map displaying travel time for 69th Street (a) and Chocolate Bayou (b).  
331 Numbers indicate travel time isochrones in minutes from the WWTP outfall (indicated with a  
332 red star).

333

### 334 **3.2. Impact of Decay Rate and Temperature on SARS-CoV-2 RNA in Transit to** 335 **Wastewater Treatment Plant**

336

337 We determined the decay rates of SARS-CoV-2 N1 and N2 at 20°C using wastewater collected  
338 from a sewershed in Houston to compare values using a Houston-specific wastewater to  
339 previously published decay rates. After the fourth day of incubation, unclear concentration  
340 dynamics occurred wherein the concentration of all targets slightly increased. Due to uncertainty  
341 in the cause of this behavior, only the first few days were considered in the regression analysis.  
342 Degradation of N1 and N2 showed similar behavior with decay rates of 0.84 day<sup>-1</sup> and 0.82 day<sup>-1</sup>,  
343 respectively. **Table S3** displays the linear regression parameters for each gene. A summary of  
344 the ddPCR droplet statistics is detailed in **Table S2**. Our experimentally-determined decay rates  
345 were within the range of published rates (**Table 1**). Decay rates listed in **Table 1** were used to  
346 evaluate the impact of decay rate and temperature on viral RNA degradation in Houston  
347 sewersheds.

348

349 **Table 1.** Summary of reported decay rates, half-lives, and  $t_{90s}$  (the time for viral concentration to  
350 decrease by one log unit) for SARS-CoV-2 RNA targets in various studies at 20°C.

Duration of Experiment (day)	Duration of Experiment (hr)	Target	Decay Rate, k (day <sup>-1</sup> )	Half Life, t <sub>1/2</sub> (day)	t <sub>90</sub> (day)	Comments	Reference
33	792	N1	0.15	4.78	15.88		Ahmed et al. 2020
1	24	N1, N2	1.75	0.40	1.31		Weidhaas et al. 2021
6	144	N1	0.84	0.83	2.74		In lab
7	168	E	0.67	0.99	3.30	High titer	Bivins et al. 2020

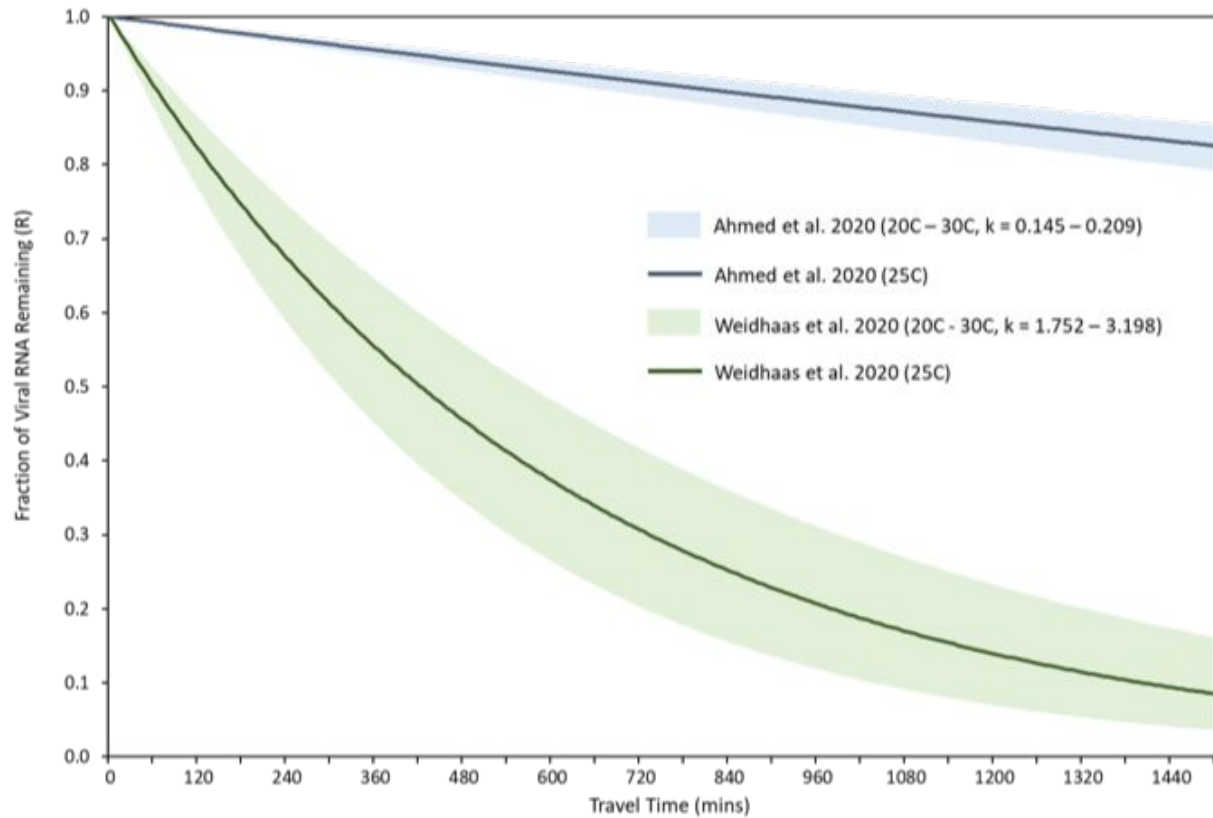
351  
352 There were significant differences in how the decay rates in **Table 1** were determined, which  
353 may explain the wide range of reported rates. Weidhaas et al. 2021 obtained the fastest decay  
354 rates compared to studies considered with a rate of (1.75 day<sup>-1</sup>) at 20°C. The authors measured  
355 SARS-CoV-2 RNA in wastewater samples obtained from two different treatment plants  
356 immediately after collection. These initial concentrations were then compared to concentrations  
357 measured in replicate samples incubated at 4, 10, and 35°C for 1 to 22 hours. Ahmed et al., 2020  
358 spiked SARS-CoV-2-negative wastewater samples with RNA extracted from gamma-irradiated  
359 SARS-CoV-2 hCoV-19/Australia/VIC01/2020 isolate and incubated them at 4, 15, 25, and 37°C  
360 over the course of 33 days in which RNA concentrations from those samples were measured  
361 every few days.

362  
363 Decay rates from Bivins et al., 2020 were the most congruent with results from our lab except  
364 under low titer conditions (starting concentration of 10<sup>3</sup> TCID<sub>50</sub> mL<sup>-1</sup>) (data not shown). The  
365 decay rate under low titer conditions was significantly slower than all other reported decay rates  
366 listed here (14). Here, the authors inoculated non-sterile wastewater with a SARS-CoV-2 isolate  
367 from a clinical patient diagnosed with COVID-19 at low titer (10<sup>3</sup> TCID<sub>50</sub> mL<sup>-1</sup>) and high titer  
368 (10<sup>5</sup> TCID<sub>50</sub> mL<sup>-1</sup>) concentrations. SARS-CoV-2 RNA was extracted and quantified in 20°C

369 inactivated wastewater samples over the course of 7 days. The decay rate associated with the  
370 high titer SARS-CoV-2 concentration was selected from the Bivins et al., 2020 study because it  
371 was more representative of concentrations previously measured in Houston sewersheds. Notably,  
372 the fastest reported decay rates from Weidhaas et al., 2021 and our own experiments were  
373 determined in samples that were not spiked with virus. This may have been due to the form of  
374 the virus in wastewater samples, which is likely a mixture of intact, protected (enveloped and/or  
375 intact capsid) virus, and degraded unprotected viral RNA. Degraded, unprotected viral RNA will  
376 degrade much faster than intact, protected virus (33). A limited number of studies have  
377 discriminated between the forms of SARS-CoV-2 in wastewater and have indicated the presence  
378 of both intact virus and free RNA (33,34). As more knowledge on factors that impact the  
379 different forms of virus becomes available, consideration should be taken when estimating or  
380 selecting SARS-CoV-2 decay rates for sewershed modeling.

381  
382 Given the ability to estimate decay rates at various temperatures for values obtained from Ahmed  
383 et al., 2020 and Weidhaas et al., 2021, and because they represented the lowest and highest decay  
384 rates reported to date, respectively, these studies were used to evaluate the effect of wastewater  
385 temperature (20-30°C) on RNA degradation over time. As expected, viral RNA degradation  
386 increases with increasing travel time. Moreover, travel time has a greater influence on  
387 degradation as compared to temperature within the range of travel times estimated for the ten  
388 sewersheds considered in this study (**Figure 4**). However, it is important to note that the impact  
389 of temperature on RNA degradation increases with increasing travel times as displayed in **Figure**  
390 **4**. For example, the difference in the percent of RNA degradation between 20 and 30°C is 0.6%

391 and 9.8% for Ahmed et al., 2020 and Weidhaas et al., 2021, respectively after a travel of 120 min  
 392 compared to 5.2% and 16% at 1200 min.



393

394 **Figure 4.** Effects of temperature, decay rate, and travel time on SARS-CoV-2 RNA degradation.

395

396 Similar findings were reported in a recent study that assessed SARS-CoV-2 RNA in sewersheds  
 397 in Tempe, Arizona under varying wastewater temperatures (16). The authors concluded that  
 398 under high temperature conditions in large sewersheds, viral concentration at outfalls may be less  
 399 representative of disease incidence as compared to colder temperatures. Wastewater  
 400 temperatures can fluctuate by as much as 27°C depending on geographical region and seasonal  
 401 changes (35). Therefore, careful consideration of wastewater temperatures can be used to

402 improve disease prevalence estimations and explain discrepancies in correlations between the  
403 number of disease cases and virus concentrations.

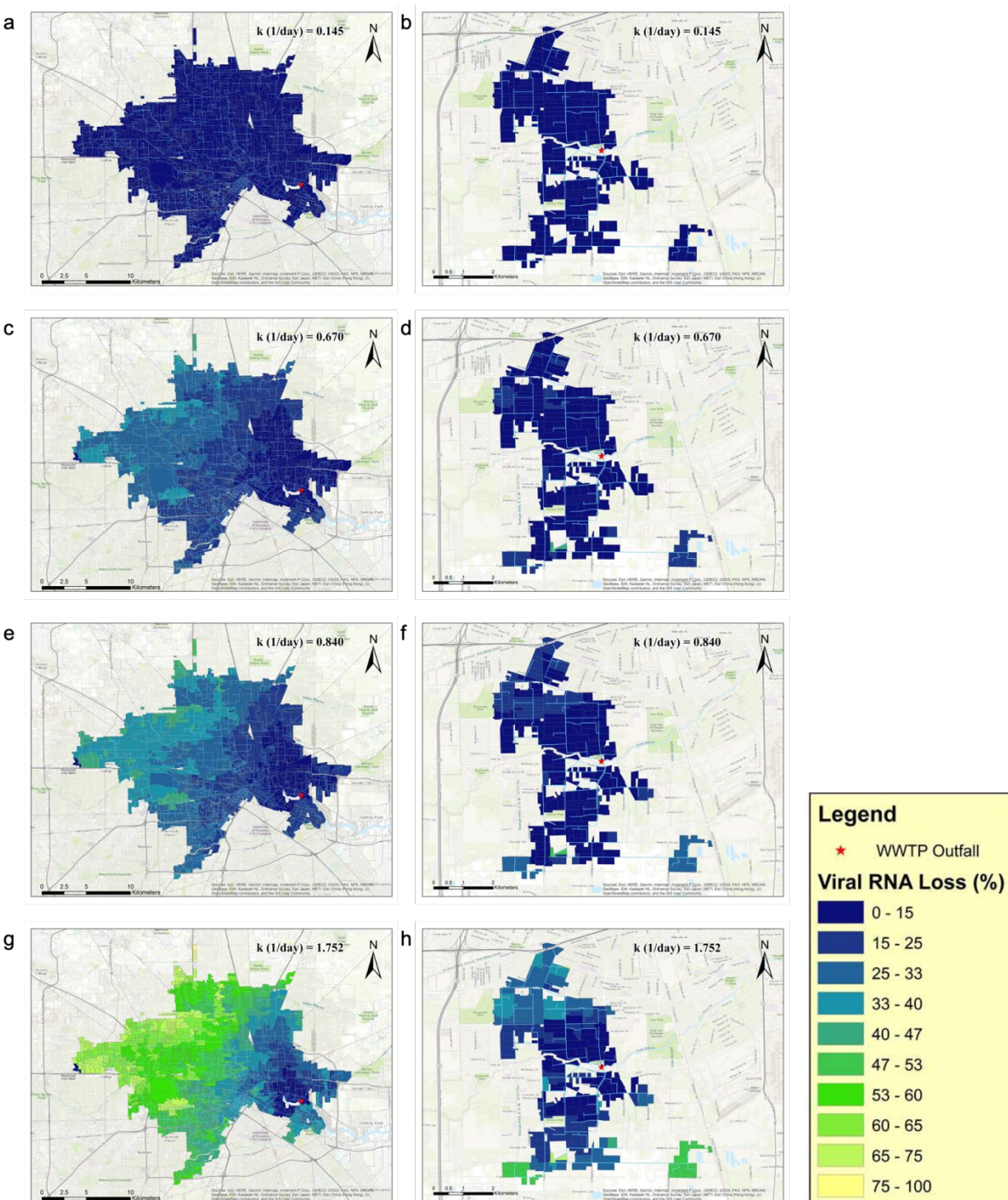
404

405 The percent of SARS-CoV-2 RNA degradation in wastewater traveling from a given  
406 geographical location within the 69th Street and Chocolate Bayou sewersheds to their  
407 corresponding outfalls at the WWTPs was determined using travel time and decay rates from  
408 **Table 1**. As expected, 69th Street showed greater variability in RNA degradation across the  
409 sewershed as compared to Chocolate Bayou. Viral RNA degradation at a median travel time of  
410 523 min for 69th Street were 5.13, 21.60, 26.29, and 47.08% for the 0.145, 0.670, 0.840, and  
411 1.752 day<sup>-1</sup> decay rates, respectively. Chocolate Bayou obtained median percent degradations of  
412 2.19, 9.73, 12.04, and 23.48% at a median travel time of 220 min (**Figure 5**). Taking into  
413 consideration the decay rate obtained from our study, approximately a 25% reduction in viral  
414 signal is estimated in the 69th Street sewershed compared to a 12% reduction for Chocolate  
415 Bayou.

416

417 Decay rates of 0.840, and 1.752 day<sup>-1</sup> resulted in SARS-CoV-2 RNA degradation of  
418 approximately  $\geq 50\%$  when considering travel times between 1190 and 570 min, respectively.  
419 Travel time range between 0-1123 min for the Chocolate Bayou sewershed, thus all regions  
420 maintained less than a 50% reduction in viral signal for a decay rate of 0.840 day<sup>-1</sup>. Despite a  
421 greater reduction of viral signal in both sewersheds when considering a virus degradation rate of  
422 1.752 day<sup>-1</sup>, the fraction of the 69th Street sewershed with  $\geq 50\%$  viral RNA degradation is  
423 49.84% as compared to 2.98% for Chocolate Bayou. Consequently, virus decay is more critical  
424 in the 69th Street sewershed due to the number of remote regions.

425



426

427



428 **Figure 5:** Geographical heat maps of SARS-CoV-2 RNA degradation for 69th Street (a, c, e, g)  
429 and Chocolate Bayou (b, d, f, h) under dry weather conditions and decay rates obtained or  
430 estimated from studies listed in Table 1.

431

### 432 **3.3. Population vs. Travel Time Metric**

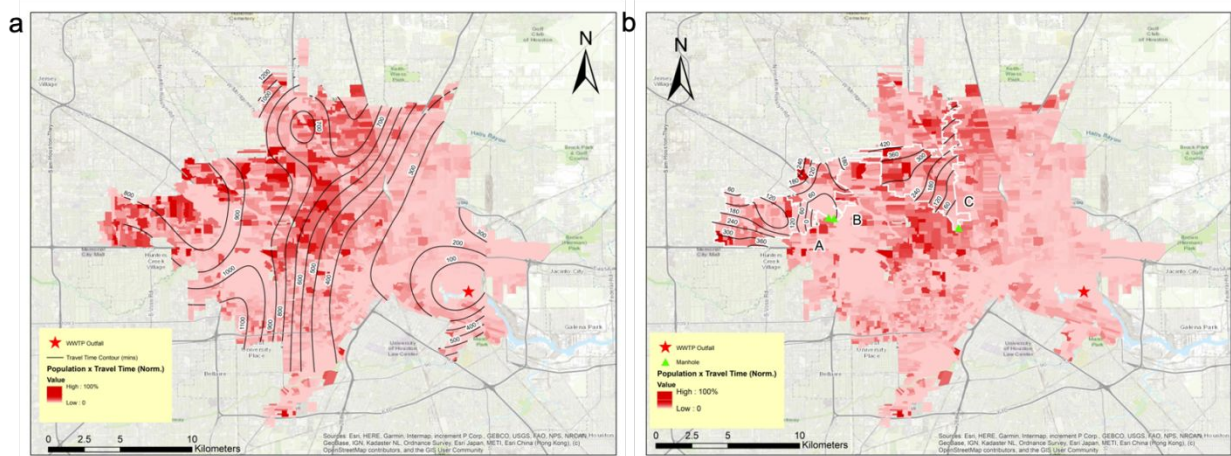
433

434 To account for virus decay across large sewersheds we propose PT, a novel metric used to  
435 facilitate the placement of upstream samplers and minimize travel times throughout sewersheds.  
436 The PT metric identifies areas that are at high risk of a wide-spread COVID-19 outbreaks due to  
437 population density and the outbreak is less likely to be fully captured in WBE due to prolonged  
438 travel times. To evaluate the efficacy of this metric, we estimated PT values for all regions  
439 within the 69th Street sewershed. **Figure 6a** illustrates a PT heatmap in the case of downstream  
440 sampling only. Hotspots were identified in the northwest-central region of the sewershed.

441

442 A second simulation was carried out with three upstream samplers hypothetically placed in  
443 hotspots (higher PT values), located in the northwest-central region, that were expected to reduce  
444 travel times in the sub-sewershed areas and minimize PT throughout the sewershed (**Figure 6b**).  
445 Placement of samplers decreased the median travel time in zones A, B, and C as indicated in  
446 **Figure 6b** from 865, 840, and 869 min to 154, 129, and 313 min, respectively. Results here  
447 indicate that implementation of upstream samplers according to the PT metric can significantly  
448 reduce the number of hotspots in large sewersheds.

449



450

451

452 **Figure 6.** (a) Display of hotspots in dark red according to normalized PT values and (b)  
 453 placement of samplers and adjusted travel times in sub-catchment zones A, B, and C in the 69th  
 454 Street sewershed.

455

#### 456 **4. Limitations and Implications**

457

458 The scope of this study does not directly take into account other factors that could influence virus  
 459 degradation such as wastewater composition and microbial predation, which could all further  
 460 explain or impact conclusions presented here. Since average travel times are approximated from  
 461 the ICM models, they may not strictly reflect transit of wastewater in the sewersheds,  
 462 particularly in remote locations and during varying diurnal cycles. Still, findings here indicate  
 463 that in-sewer decay may be an important factor to consider in WBE and when designing  
 464 sampling campaigns.

465

#### 466 **5. Conclusion**

467

468 A hydraulic modeling approach was applied to 10 Houston sewersheds to estimate travel times  
469 and decay of SARS-CoV-2 from source to the WWTP outfall under various temperatures. Travel  
470 time generally had a greater impact on viral RNA degradation than wastewater temperature. The  
471 largest sewershed showed greater variability in viral RNA degradation due to longer travel times  
472 with nearly half of the sewershed losing 50% or more of the viral signal when considering the  
473 fastest decay rate. By incorporating a novel PT metric for placement of upstream samplers within  
474 the largest sewershed, travel times reduced by more than 60%. This reduction is expected to  
475 alleviate virus signal loss due to decay and discrepancies between wastewater and clinical cases  
476 in wastewater surveillance efforts. This approach can be adopted in various localities to improve  
477 sampling infrastructures and public health responses to local and global viral disease outbreaks.

478

#### 479 **Conflicts of interest**

480 There are no conflicts to declare.

481

#### 482 **Acknowledgment**

483 A special thanks to Houston Public Works for providing ICM models for selected sewersheds  
484 and additional sewershed characteristics where needed. We'd also like to thank the Houston  
485 Health Department, and specifically Courtney Hundley, Rebecca Schneider, and Lilian Mojica,  
486 for providing aggregate travel times for positive COVID-19 cases as needed. We thank Prashant  
487 Kalvapalle for his contribution to the wastewater-based epidemiology method development  
488 along with the Lauren Stadler and Anthony Maresso lab groups at Rice University and Baylor  
489 College of Medicine for their assistance with wastewater sample collection, processing, and  
490 analysis.

## 491 **Funding Sources**

492 This work was supported by the Houston Health Department and grants from the National  
493 Science Foundation (CBET 2029025) and seed funds from Rice University. Z.W.L. was funded  
494 by an Environmental Research & Education Foundation scholarship.

495

## 496 **References**

497

- 498 1. Bisseux M, Colombet J, Mirand A, Roque-Afonso AM, Abravanel F, Izopet J, et al.  
499 Monitoring human enteric viruses in wastewater and relevance to infections encountered  
500 in the clinical setting: A one-year experiment in central France, 2014 to 2015.  
501 *Eurosurveillance*. 2018;23(7):1–11.
- 502 2. Brouwer AF, Eisenberg JNS, Pomeroy CD, Shulman LM, Hindiyeh M, Manor Y, et al.  
503 Epidemiology of the silent polio outbreak in Rahat, Israel, based on modeling of  
504 environmental surveillance data. *Proceedings of the National Academy of Sciences of the*  
505 *United States of America*. 2018 Nov 6;115(45):E10625–33.
- 506 3. Kamel AH, Ali MA, El-Nady HG, Aho S, Pothier P, Belliot G. Evidence of the co-  
507 circulation of enteric viruses in sewage and in the population of Greater Cairo. *Journal of*  
508 *Applied Microbiology*. 2010;
- 509 4. Kokkinos P, Ziros P, Meri D, Filippidou S, Kolla S, Galanis A, et al. Environmental  
510 surveillance. An additional/alternative approach for virological surveillance in Greece?  
511 *International Journal of Environmental Research and Public Health*. 2011;8(6):1914–22.
- 512 5. la Rosa G, della Libera S, Iaconelli M, Ciccaglione AR, Bruni R, Taffon S, et al.  
513 Surveillance of hepatitis A virus in urban sewages and comparison with cases notified in  
514 the course of an outbreak, Italy 2013. *BMC Infectious Diseases*. 2014;14(1):1–11.
- 515 6. Parasa S, Desai M, Thoguluva Chandrasekar V, Patel HK, Kennedy KF, Roesch T, et al.  
516 Prevalence of Gastrointestinal Symptoms and Fecal Viral Shedding in Patients with  
517 Coronavirus Disease 2019: A Systematic Review and Meta-analysis. Vol. 3, *JAMA*  
518 *Network Open*. American Medical Association; 2020.
- 519 7. la Rosa G, Mancini P, Bonanno Ferraro G, Veneri C, Iaconelli M, Bonadonna L, et al.  
520 SARS-CoV-2 has been circulating in northern Italy since December 2019: Evidence from  
521 environmental monitoring. *Science of the Total Environment*. 2021 Jan 1;750.
- 522 8. Randazzo W, Truchado P, Cuevas-Ferrando E, Simón P, Allende A, Sánchez G. SARS-  
523 CoV-2 RNA in wastewater anticipated COVID-19 occurrence in a low prevalence area.  
524 *Water Research*. 2020 Aug 15;181.
- 525 9. Stadler LB, Ensor KB, Clark JR, Kalvapalle P, LaTurner ZW, Mojica L, et al. Wastewater  
526 Analysis of SARS-CoV-2 as a Predictive Metric of Positivity Rate for a Major Metropolis.  
527 *medRxiv*. medRxiv; 2020.

- 528 10. Wu F, Zhang J, Xiao A, Gu X, Lee WL, Armas F, et al. SARS-CoV-2 Titers in  
529 Wastewater Are Higher than Expected from Clinically Confirmed Cases. *mSystems*. 2020  
530 Jul 21;5(4).
- 531 11. Ahmed W, Tscharke B, Bertsch PM, Bibby K, Bivins A, Choi P, et al. SARS-CoV-2 RNA  
532 monitoring in wastewater as a potential early warning system for COVID-19 transmission  
533 in the community: A temporal case study. *Science of the Total Environment*. 2021 Mar  
534 20;761.
- 535 12. Xagorarakis I. Can We Predict Viral Outbreaks Using Wastewater Surveillance? *Journal of*  
536 *Environmental Engineering*. 2020;146(11):01820003.
- 537 13. Weidhaas J, Aanderud ZT, Roper DK, VanDerslice J, Gaddis EB, Ostermiller J, et al.  
538 Correlation of SARS-CoV-2 RNA in wastewater with COVID-19 disease burden in  
539 sewersheds. *Science of the Total Environment*. 2021 Jun 25;775.
- 540 14. Bivins A, Greaves J, Fischer R, Yinda KC, Ahmed W, Kitajima M, et al. Persistence of  
541 SARS-CoV-2 in Water and Wastewater. *Environmental Science and Technology Letters*.  
542 2020 Dec 8;7(12):937–42.
- 543 15. Ahmed W, Angel N, Edson J, Bibby K, Bivins A, O'Brien JW, et al. First confirmed  
544 detection of SARS-CoV-2 in untreated wastewater in Australia: A proof of concept for the  
545 wastewater surveillance of COVID-19 in the community. *Science of the Total*  
546 *Environment*. 2020;
- 547 16. Hart OE, Halden RU. Computational analysis of SARS-CoV-2/COVID-19 surveillance by  
548 wastewater-based epidemiology locally and globally: Feasibility, economy, opportunities  
549 and challenges. *Science of the Total Environment*. 2020 Aug 15;730.
- 550 17. Hong PY, Rachmadi AT, Mantilla-Calderon D, Alkahtani M, Bashawri YM, al Qarni H,  
551 et al. Estimating the minimum number of SARS-CoV-2 infected cases needed to detect  
552 viral RNA in wastewater: To what extent of the outbreak can surveillance of wastewater  
553 tell us? *Environmental Research*. 2021 Apr 1;195.
- 554 18. Gundy PM, Gerba CP, Pepper IL. Survival of Coronaviruses in Water and Wastewater.  
555 *Food and Environmental Virology*. 2009 Mar 1;1(1):10–4.
- 556 19. Matus M, Duvallet C, Soule MK, Kearney SM, Endo N, Ghaeli N, et al. 24-hour multi-  
557 omics analysis of residential sewage reflects human activity and informs public health.  
558 *bioRxiv*. 2019;
- 559 20. Larson RC, Berman O, Nourinejad M. Sampling manholes to home in on SARS-CoV-2  
560 infections. *PLoS ONE*. 2020 Oct 1;15(10 October).
- 561 21. Yeager RA, Holm RH, Saurabh K, Fuqua JL, Talley D, Bhatnagar A, et al. Wastewater  
562 sample site selection to estimate geographically-resolved community prevalence of  
563 COVID-19: A research protocol. *medRxiv*. medRxiv; 2020.
- 564 22. Acosta N, Bautista MA, Hollman J, McCaldler J, Beaudet AB, Man L, et al. A multicenter  
565 study investigating SARS-CoV-2 in tertiary-care hospital wastewater. viral burden  
566 correlates with increasing hospitalized cases as well as hospital-associated transmissions  
567 and outbreaks. *Water Research*. 2021 Aug 1;201.
- 568 23. Schmitz BW, Innes GK, Prasek SM, Betancourt WQ, Stark ER, Foster AR, et al.  
569 Enumerating asymptomatic COVID-19 cases and estimating SARS-CoV-2 fecal shedding  
570 rates via wastewater-based epidemiology. *Science of the Total Environment*. 2021 Dec  
571 20;801.

- 572 24. Haak L, Delic B, Li L, Guarin T, Mazurowski L, Dastjerdi NG, et al. Spatial and temporal  
573 variability and data bias in wastewater surveillance of SARS-CoV-2 in a sewer system.  
574 *Science of the Total Environment*. 2022 Jan 20;805.
- 575 25. Sy KTL, White LF, Nichols BE. Population density and basic reproductive number of  
576 COVID-19 across United States counties. *PLoS ONE*. 2021 Apr 1;16(4 April).
- 577 26. Coşkun H, Yıldırım N, Gündüz S. The spread of COVID-19 virus through population  
578 density and wind in Turkey cities. *Science of the Total Environment*. 2021 Jan 10;751.
- 579 27. Peng HQ, Liu Y, Wang HW, Ma LM. Assessment of the service performance of drainage  
580 system and transformation of pipeline network based on urban combined sewer system  
581 model. *Environmental Science and Pollution Research*. 2015 Oct 1;22(20):15712–21.
- 582 28. LaTurner ZW, Zong DM, Kalvapalle P, Gamas KR, Terwilliger A, Crosby T, et al.  
583 Evaluating recovery, cost, and throughput of different concentration methods for SARS-  
584 CoV-2 wastewater-based epidemiology. *Water Research*. 2021 Jun 1;197.
- 585 29. R Core Team. R: A language and environment for statistical computing. Vienna, Austria  
586 [Internet]. 2020 [cited 2021 Sep 28]; Available from: <https://www.r-project.org/>
- 587 30. Blaustein RA, Pachepsky Y, Hill RL, Shelton DR, Whelan G. *Escherichia coli* survival in  
588 waters: Temperature dependence. *Water Research*. 2013 Feb 1;47(2):569–78.
- 589 31. Behradek. Temperature Coefficients in Biology. *Biological Reviews*. 1930;5:30–59.
- 590 32. Reyes BA, Pendergast JS, Yamazaki S. Mammalian Peripheral Circadian Oscillators Are  
591 Temperature Compensated NIH Public Access. Vol. 23, *J Biol Rhythms*. 2008.
- 592 33. Wurtzer S, Waldman P, Ferrier-Rembert A, Frenois-Veyrat G, Mouchel JM, Boni M, et  
593 al. Several forms of SARS-CoV-2 RNA can be detected in wastewaters: Implication for  
594 wastewater-based epidemiology and risk assessment. *Water Research*. 2021  
595 Jun;198:117183.
- 596 34. Canh VD, Torii S, Yasui M, Kyuwa S, Katayama H. Capsid integrity RT-qPCR for the  
597 selective detection of intact SARS-CoV-2 in wastewater. *Science of the Total  
598 Environment*. 2021 Oct 15;791.
- 599 35. Hart OE, Halden RU. Modeling wastewater temperature and attenuation of sewage-borne  
600 biomarkers globally. *Water Research*. 2020 Apr 1;172.

602